

# Two-Dimensional Materials for Future Terahertz Wireless Communications

ABDOALBASET ABOHMRA<sup>1</sup> (Student Member, IEEE), ZIA ULLAH KHAN<sup>1</sup> (Student Member, IEEE),  
HASAN T. ABBAS<sup>1</sup> (Senior Member, IEEE), NOSHERWAN SHOAB<sup>2</sup> (Senior Member, IEEE),  
MUHAMMAD A. IMRAN<sup>1</sup> (Senior Member, IEEE), AND QAMMER H. ABBASI<sup>1</sup> (Senior Member, IEEE)

<sup>1</sup>James Watt School of Engineering, University of Glasgow, Glasgow G12 8QQ, U.K.

<sup>2</sup>Research Institute for Microwave & Millimeter Wave Studies, National University of Sciences and Technology (NUST), Islamabad 44000, Pakistan

CORRESPONDING AUTHOR: Q. H. ABBASI (e-mail: qammer.abbasi@glasgow.ac.uk)

This work was supported by the Engineering and Physical Sciences Research Council EPSRC IAA under Grant EP/R511705/1.

**ABSTRACT** The high bandwidth and data rate demands of future wireless communications such as 6G and beyond can no longer be met with existing technologies that are mainly based on naturally occurring three-dimensional materials. The terahertz (THz) band refers to the electromagnetic frequency range lying between the millimetre-wave band and the infrared band, and it has become an increasingly promising frequency band that has the potential to be exploited for high-speed wireless communication networks of the future. Lately, the realisation of THz devices has been expedited through the emergence of two-dimensional materials (2DMs), such as graphene, perovskites, and transition metal dichalcogenides that can potentially unlock some long-standing problems related to the development of efficient control of transmission and detection of THz waves. In this paper, we cover several essential electrical features of 2DM, namely graphene, MOs<sub>2</sub>, and perovskite enabled THz devices that are being used to design efficient systems for future wireless communication systems.

**INDEX TERMS** Terahertz, two-dimensional materials, wireless communications, 6G, graphene, perovskites.

## I. INTRODUCTION

THE TERAHERTZ (THz) frequency region lies between 100 GHz ( $\lambda = 3$  mm) to 10 THz ( $\lambda = 30$   $\mu$ m). Notably, the atmospheric absorption in the THz frequency region is high, which delays the application of THz waves for long-distance communications [1], [2], [3]. Through existing THz technologies out of which devices such as detectors and sources are made, measurements at distances more than 20 m become challenging. On the other hand, short-range communications are becoming increasingly attractive modes for sharing information. According to Edholm's law, the requirement for point-to-point bandwidth in short-range wireless communications grows every 18 months [4], [5]. As the data rate is typically proportional to the central frequency of the communication system, researchers from academia and

industry have been encouraged to investigate the unexploited electromagnetic spectrum between the microwave and optics region to reap the benefits of high bandwidth systems. Transmitters, detectors, and modulator are essential for the integration of any communication system and same is for the THz technologies [6]. However, for the effective wireless communication in the THz band, various radiofrequency (RF) components such as signal sources, detectors, modulators and amplifiers need to be improved. Additionally, most standard materials normally utilized at microwave frequency are highly inefficient in the THz frequency range. Copper is a frequently used metal in radio frequency (RF) and microwave device fabrication. Metal design has been widely researched in the RF and microwave frequency bands, and systematic design methodologies are presented in the Balanis foams

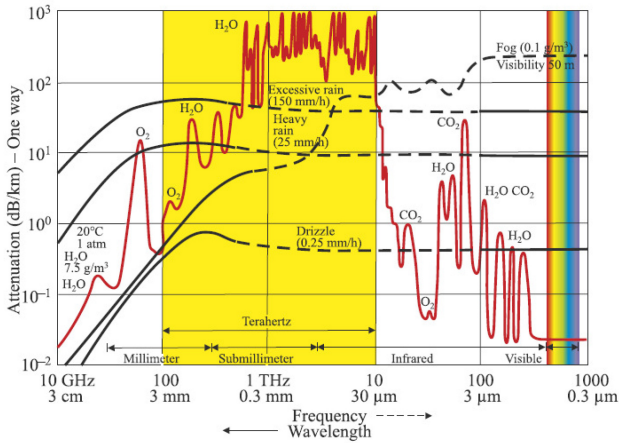


**FIGURE 1.** Propagation of THz in the air [2]. The radiation has to be within an atmospheric transmission window to prevent high water vapour absorption.

book [7]. Few high-directivity metal THz antenna and array topologies, including planar antennas and arrays, have been developed during the past several decades [8], [9], [10]. However, The THz copper metal antenna is not the same as a microwave metal antenna. THz antennas are excited by lasers through fibre or air, while traditional microwave metal antennas are excited via a microstrip coaxial cable, or CPW [11]. THz antennas need bias voltage, while microwave antennas do not. Graphene, the most recent carbon-based nanomaterial, has a greater current density and electron mobility than common metals such as copper [12], [13]. Conventional materials are not suitable for RF applications such as electrical interconnects and radiating components operating in the THz band due to their very small size of a few micrometers combined with an exceptionally high resistance per unit length [14]. Additionally, since the surface resistivity of conventional conductors rises with frequency owing to the skin depth effect, the radiation effectiveness of nano-radius wire antennas is very poor due to the substantial ohmic losses associated with these diameters [15].

An important advancement in developing materials and device design has been made at this frequency range. Despite the substantial progress in THz device work recently THz applications are still in the initial stages of development. As a result, numerous additional potential applications can be added to healthcare, short-range wireless communications, safety, food quality detection, spectroscopic analysis [2], [4], [16], [17], [18].

Functional materials are now considered as the fundamental building blocks for the realisation of THz devices [19]. In this regard, 2DMs such as hexagonal boron nitride (h-BN), transition metal dichalcogenides (TMD)s, graphene, and perovskites family have gained more consideration for THz applications [20]. 2DMs are characteristically described as single-layer materials that have become a central research point ever since the emergence of graphene. A

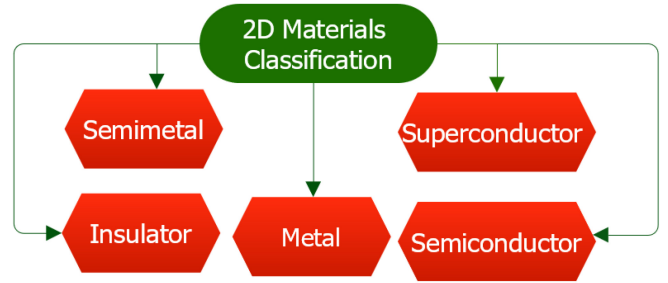


**FIGURE 2.** The two-dimensional material family.

particular crystal form and nuclear layer stacking sequence, particularly in TMDs, can result in vastly different physical properties such as superconductors, metal, insulator, and semiconductor [21]. The family of 2DMs shows a widespread series of novel mechanical and electrical properties, for instance thermal stability, bandgap tunability, and high conductivity [22]. Moreover, in stark contrast with their bulk counterparts, one of the fascinating features of 2DMs is the ultra-high specific surface areas that enable their energy construction vulnerable to voltage biasing [23]. However, there are numerous other 2DMs that remain undiscovered. Furthermore, combining different 2DMs results in new structures with unique physical and concoction properties [24].

2DMs also enable the development of sensing systems that can be tuned through the electronic band structure by controlling their thickness and amount of dopants, alloying between various materials [25]. Metals, such as gold and copper regularly show surface plasmon polaritons (SPP) in the optical frequency range, but have vastly different physical properties in the THz band effecting their performance [26], [27], [28]. As the THz resonance is far beneath the aforementioned metals' plasma frequencies, these materials have high conductivity which causes them to behave as a perfect electric conductor (PEC) to a more prominent degree [26]. In this manner, the SPP's electric field just enters the metal, showing poor repression, accordingly, losing a lot of points of interest [29].

Additional line of research pries the field wide open as the exploration of new functional 2DMs and experimentally accessible 2DMs grow at a rapid pace, such a diverse family encompasses a large variety of material properties including insulators, semiconductors, semimetals, and metals as shown in Fig. 2. An exciting aspect of 2DMs is to get benefit of the greatly unique properties of and load them into a configuration to make new THz devices created from ultra-thin elements [31]. Every 2DM identified or to be realized might consequently offer a new application for THz waves [32], [33], [34], [35]. Here, we mainly show the properties of several 2DMs including graphene, TMDs and Perovskite and their usages in the THz communication. Using the 2D material characteristics for terahertz wireless application, we outline the operating concept in Section II. Two-dimensional materials are defined, as are

their characteristics and structure. Section III summarizes the electronic characteristics of 2d materials, including the tuning properties of graphene plasmons, mos2, and perovskite in the terahertz region. Several terahertz applications, ranging from modulators to source to detectors, are discussed in Section III.

## II. 2DM ELECTRONIC PROPERTIES

In the scope of 100 GHz to 1 THz frequency range, the wavelength ranges from  $10^8$  to  $10^5$  nm, which is exceptionally short [36]. The skin depth is a convenient method to identify the radius of a metal in which the majority of the current is flowing. It is unnecessary to use a wire with a radius that is considerably greater than the skin depth since the current moves in the skin-depth area regardless of the conductor size [36], [37], [37]. Due to its unique structural and physical properties (Fig. 5 (a)), h-BN is considered a potential assistance material for improving the electrical and optoelectronic performance of other 2D materials [38], [39]. Furthermore, graphene/h-BN heterostructure offers a platform for researching many-body correlation phenomena of Dirac fermions, such as the fractional quantum Hall effect in the high magnetic field of graphene [40], [41]. h-BN has also been discovered to be useful in other areas [41], [42], including carrier tunneling and deep ultraviolet optoelectronics [43].

### A. THZ GRAPHENE PLASMONICS

Because of the skin depth effect, the surface resistivity of typical conductors rises with frequency for conventional metals, and so the radiation efficiency of nano-radius antennas is relatively poor owing to substantial ohmic losses at very tiny scales [14], [36]. As a result, it is probable that the 2DMs will surpass traditional metal-based antennas in terms of radiation efficiency [44].

SPPs are electromagnetic waves that propagate along the surface of a conductor [45]. These waves produced in the structure of collective oscillations of electrons allow the sequestration and management of electromagnetic power at subwavelength scales [46]. SPPs are extremely sensitive to slight agitation in the skin depth. Graphene has a significantly lower  $\omega$  than Gold by an order of two in magnitude as illustrated in Fig. 3. A single graphene layer can support a SPPs on it. The propagation length is at best of the order of one SPP wavelength for deeply biased graphene in the infrared band.

Graphene supports the propagation of SPPs that are with no substantial loss, and more importantly, it exhibits the excellent property of being tunable through electrical/magnetic bias or synthetic doping [47], [48]. Zero-bias thermoelectric photodetectors based on a single graphene sheet produced by chemical vapour deposition were used to tune throughout the whole terahertz range from 0.1 to 10 THz (CVD) [49]. Biased graphene with dielectric constants of  $\epsilon_1$  and  $\epsilon_2$  and the collective oscillations in graphene are

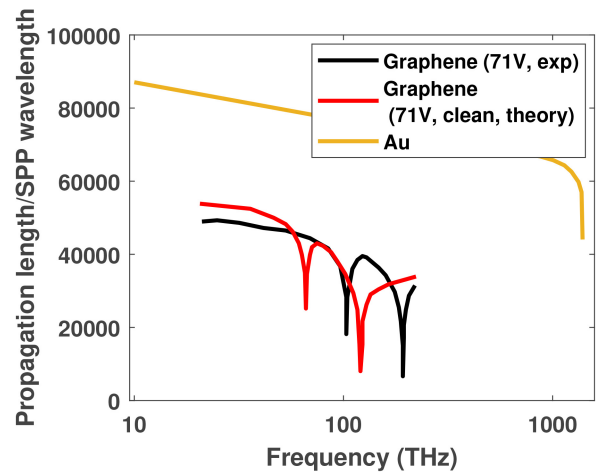


FIGURE 3. Comparison of graphene and gold plasmonic characteristics, adapted from [30].

stirred up by electromagnetic waves of transverse magnetic approach, the dispersion described as [50].

$$k_{spp} = \epsilon_0 \frac{\epsilon_1 + \epsilon_2}{2} \frac{2i\omega}{\sigma(\omega, q)} \quad (1)$$

where  $k_{spp}$  is a complex, the real part is the corresponding to the plasmonic wave, and the imaginary part is the decay. Where plasmonic wave can be accomplished in the far infrared as the large imaginary conductivity and small Ohmic loss in the real part. However, in the infrared frequency region, the plasmonic wavelengths can increase to 100. The plasmons on graphene can be manipulated by optical pumping, doping, and electrostatic gating. Graphene's conductivity can be modeled in the THz band using the Kubo formula [55].

$$\sigma = \frac{2e^2 k_B T}{\pi \hbar^2 (\omega - j\tau^{-1})} \ln \left\{ 2 \left[ 1 + \cosh \left( \frac{\mu_c}{k_B T} \right) \right] \right\} + \frac{e^2}{4\hbar} \left( \frac{1}{2} + \frac{1}{\pi} \tan^{-1} \left( \frac{\hbar\omega - 2\mu_c}{2k_B T} \right) - \frac{i}{2\pi} \ln \left( \frac{(\hbar\omega - 2\mu_c)^2}{(\hbar\omega - 2\mu_c)^2 + 4(k_B T)^2} \right) \right) \quad (2)$$

where the scattering time is  $\tau$ , the Boltzmann constant is  $k_B$ , the electron charge is  $e$ , the temperature is  $T$ , the Planck constant is  $\hbar$ , the angular frequency is  $\omega$ , and the chemical potential is  $\mu_c$ . The conductivity of graphene regulates its reactivity using a chemical potential and relaxation time that can be calculated by, [56],

$$\mu_c = \hbar v_f \sqrt{\pi n} \quad (3)$$

$$\tau = \frac{\mu_c \mu}{e v_f^2} \quad (4)$$

where  $v_f$  is the Fermi velocity ( $10^6$  s/m),  $n$  is the carrier density and  $\mu$  is the carrier mobility of the electrons. Frequency changing and a wide bandwidth can be accomplished by changing the chemical potential and scattering

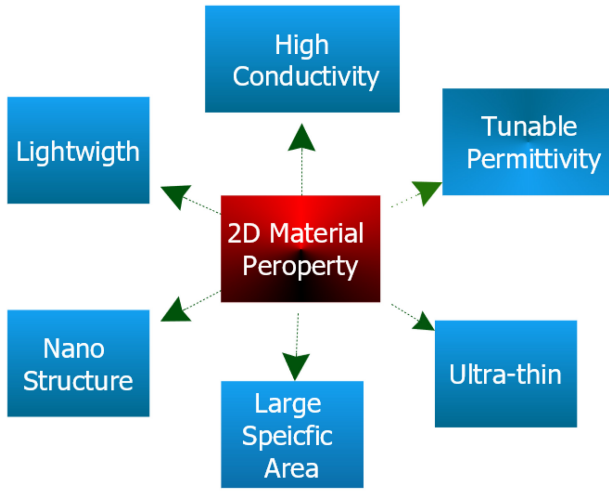


FIGURE 4. 2DMs Property.

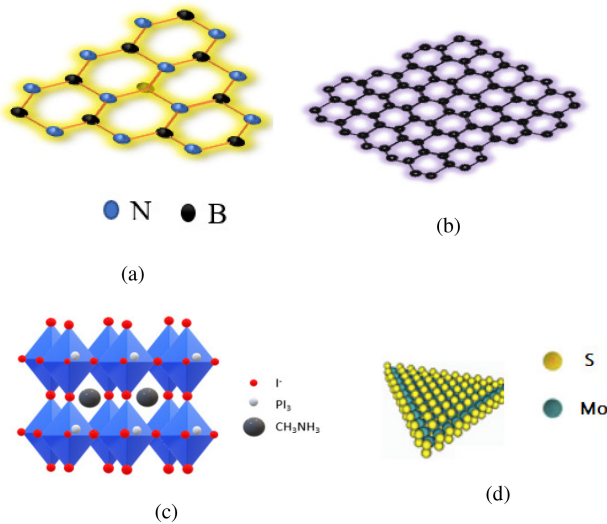


FIGURE 5. The 2DM structure: (a) hexagonal boron nitride (h-BN) (b) Graphene (c) Perovskite  $\text{CH}_3\text{NH}_3\text{PbI}_3$  (d) Molybdenum disulphide ( $\text{MoS}_2$ ).

time. However, increasing chemical potential affects the radiation from graphene as the absorption level will increase. An important characteristic of the graphene band structure is that under zero doping conditions the chemical potential remains along with the Dirac point and thus there are only a few available free electrons. Any change in position of the chemical potential,  $\mu$ , can have drastic consequences on the free carrier density of the system. In extremely low  $\mu$  and carrier mobility, invalid force reactions are found. This suggests that reverberation is not achieved due to the attenuation of SPPs as they spread on the graphene surface. Even though the rise of the  $\mu$  and the carrier mobility support the radiated energy, they have their effect on the impulse response. However, the increase in the  $\mu$  and the carrier mobility affects the width of the response (bandwidth) [57]. It has been emphasized the relevance of intraband and interband contributions to surface

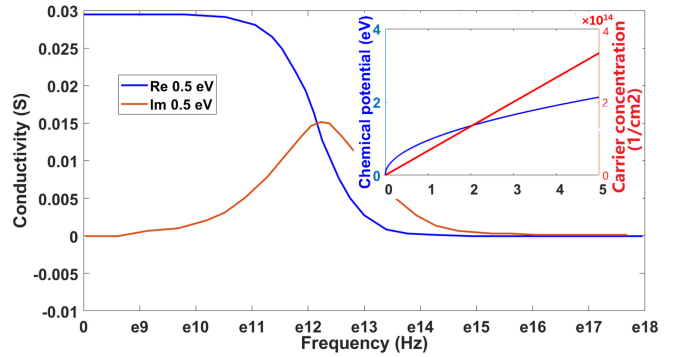
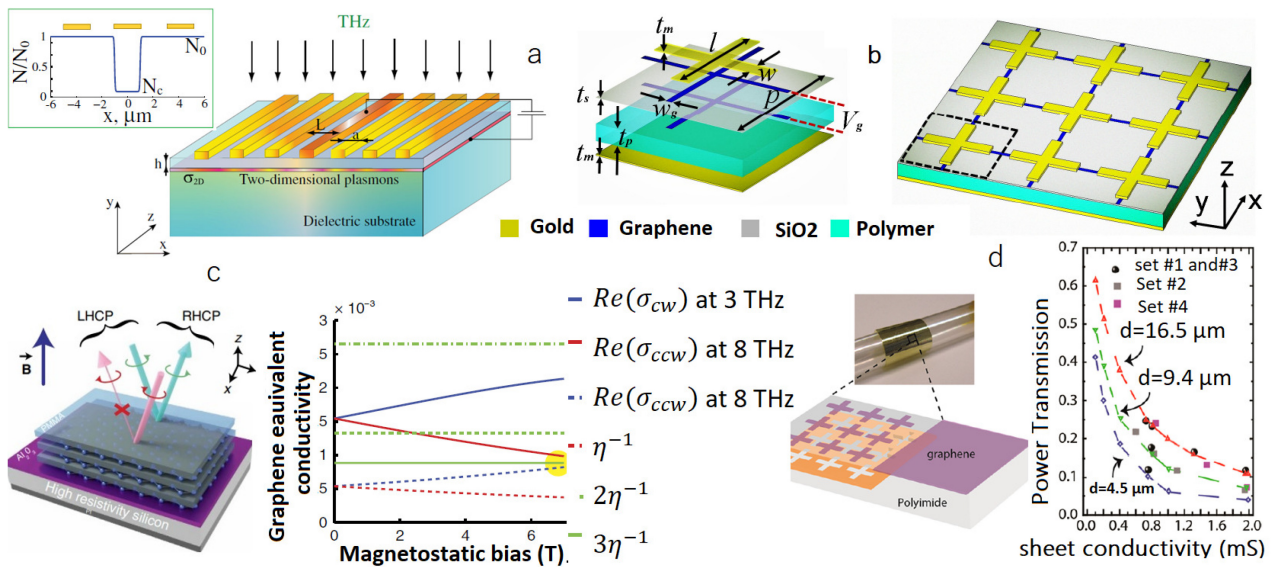


FIGURE 6. Real and imaginary conductivity of graphene.

wave propagation [58]. The intraband conductivity can be adjusted by modifying the chemical potential at infrared frequencies, allowing for certain control over surface wave characteristics. According to [59], a transverse electromagnetic mode may be adjusted from radio to infrared by altering the density of charge carriers in graphene through a gate voltage.

Plasmonic in graphene with many more attractive properties like high carrier mobility, low gate voltage, and nanostructure shows an excellent capability for THz resonant devices operating in the THz frequency range. The Electric field effect variation of electron density and generate periodic plasmonic lattices with a defect cavity introduced in [51]. In addition, deeply pumped cavity plasmon types are excited in a periodic plasmonic lattice by an incident THz radiation causing a deep subwavelength concentration of THz energy (Fig. 7(a)). A great field enhancement of two orders of magnitude is better than the value in conventional metals at THz. Another important feature of graphene is that graphene can be used in creating tunable THz devices. A cross-shaped metamaterial containing a two-layer of graphene was designed for accomplishing a tunable polarization absorber, as shown in Fig. 7 (b). The absorption was performed with the highest frequency tuning range of 15%. The peak absorption has been determined by regulating the Fermi energy which can be accomplished by changing the bias voltage. The device can turn the reflected wave through a linear polarization of the tunable azimuth angle from  $0^\circ$  to  $90^\circ$  at the operating frequency [52].

A THz nonreciprocal isolator with circular polarization based on biased graphene has been introduced in [53]. The isolator displays nearly 20 dB isolation and 7.5 dB insertion loss at 2.9 THz (Fig. 7 (c)). The hybrid graphene metamaterial paves the way for actively manipulating the mutual interaction of THz waves and matter at the deep subwavelength scale and enabling a variety of THz applications such as tunable memory devices and modulators [54] (Fig. 7 (d)). Another sort of THz modulator has been developed, which utilises a frequency selective surface to resonantly boost graphene's THz response.



**FIGURE 7.** Graphene-based THz devices and THz graphene plasmonics. (a) A split grating gate field effect transistor [51]. (b) Diagram of graphene plasmon nonlinear absorption [52]. (c) Metamaterial modulator made of graphene [53]. The top of the polyimide substrate is covered with nonpatterned and patterned graphene layers. (d) A diagram of the graphene metamaterial absorber's structure in [54].

### B. PEROVSKITE AND MOS<sub>2</sub> THZ PROPERTIES

Perovskites have been extensively examined in the field of THz application given their appealing properties [60], [61], however, perovskite application is usually limited to photovoltaic and solar domains. The properties of perovskite family materials have allowed the development of many novel devices and applications. Perovskite materials reveal several exceptional physical characteristics such as ferroelectricity, superconductivity, and high thermopower [62]. Perovskite were discovered by Weber in 1978 [63]. However, CH<sub>3</sub>NH<sub>3</sub>PbI<sub>3</sub> perovskite has been recognized as promising material due to its high charge carrier mobility, and diffusion length indicating that this material could be a potential candidate for THz application (Fig. 5 (c)). However, adjusting the physical property in this material is very tricky [64]. CH<sub>3</sub>NH<sub>3</sub>PbI<sub>3</sub> is a perovskite structure, which is combined of one Pb<sup>2+</sup>, one CH<sub>3</sub>NH<sub>3</sub><sup>+</sup>, with three iodine anions in the unit cell. Therefore, lead iodide perovskite precursor solution can be made by combining the CH<sub>3</sub>NH<sub>3</sub>I and PbI<sub>2</sub> at 15:1 molar ratios to meet the atom ratio in CH<sub>3</sub>NH<sub>3</sub>PbI<sub>3</sub> [65]. This material could have a potential high efficiency in THz frequency [66]. The complex photoconductivity  $\Delta\tilde{\sigma}(\omega, \tau)$  is the sum of Drude and Smith conductivities in the Drude-Smith model [67], [68].

$$\Delta\tilde{\sigma}(\omega, \tau) = \frac{\varepsilon_0\omega_p^2}{\Gamma - i\omega} \left[ 1 + \frac{c_1}{1 - i\omega/\Gamma} \right] \quad (5)$$

where the first term  $\Delta\tilde{\sigma}_{(D-S)} = \varepsilon_0\omega_p^2/(\Gamma - i\omega)$  is the Drude conductivity. The second Smith term  $c_1\Delta\tilde{\sigma}_D/(1 - i\omega/\Gamma)$ .

Figures 8 and 9 show the permittivity and conductivity of at 300 K for CH<sub>3</sub>NH<sub>3</sub>PbI<sub>3</sub>. At low frequencies, the dielectric constant is large; it has been reported to be 60.9

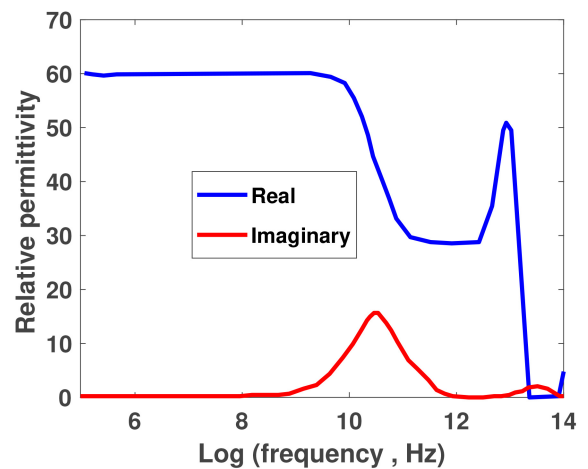


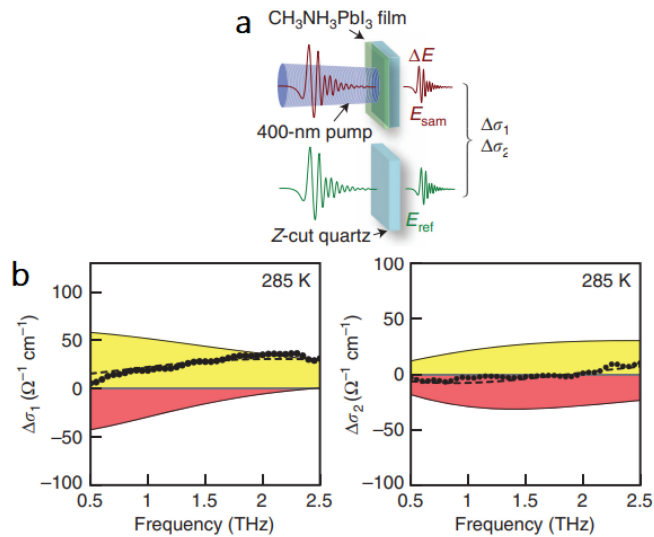
**FIGURE 8.** Permittivity and conductivity of CH<sub>3</sub>NH<sub>3</sub>PbI<sub>3</sub> perovskite ([65]).

over the 20 Hz – 1MHz range, which is consistent with the low frequency value of 60 obtained from fits at higher frequencies. This low-frequency value is appropriate in determining steady-state properties, with static fields consequently varying slowly with position five times slower than in silicon under similar electrostatic disturbances. At infrared frequencies, the ionic component drops out, leaving only the electronic response. The dielectric constant drops to 6.5 at optical frequencies, lower than that of inorganic semiconductors with a similar bandgap [82]. The other possibility is that CH<sub>3</sub>NH<sub>3</sub>PbI<sub>3</sub> may possess paraelectric or even ferroelectric properties at room temperature and above [65].

Coating the perovskite material on a wafer allows the modulation of THz band at 50 GHz modulating speed. Therefore, the ultrafast response opens the excellent potential in flexible

**TABLE 1.** THz uses of two-dimensional materials: graphene and beyond.

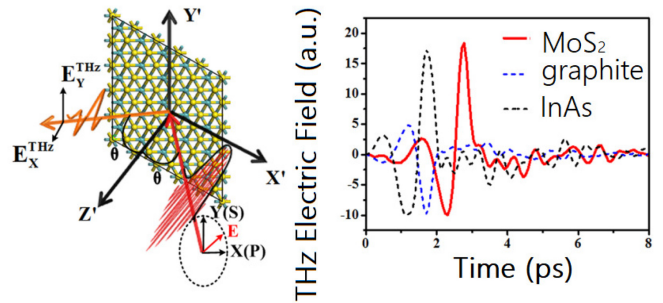
| Material   | Fundamental properties                              | Frequency of operation | Usage in THz wireless communication   |
|------------|---|------------------------|---|
| Graphene   | Surface plasmon propagation. Ultra-thin Flexibility | 0.1 to 10THz           | Antenna [69] [70], absorption [71], metasurface [72], detection [73],and modulation [74]              |
| Mos2       | SPP, high conductivity, Ultra-thin                  | 0.1 to 10THz           | Modulation [75] [26], Enhanced terahertz emission [76], and tunable terahertz broadband absorber [77] |
| Perovskite | Ferroelectricity, Superconductivity                 | 0.1 to 10THz           | Antenna [78], Modulation [79] [80]  |
| h-BN       | Tunnelling and deep ultraviolet optoelectronics     | 0.1 to 10THz           | used in conjunction with other 2D materials to improve performance [81] [38] [39]                     |


**FIGURE 9.** (a) THz transient of the  $\text{CH}_3\text{NH}_3\text{PbI}_3$  thin film after optical excitation with 400 – nm pump pulses with a fluence of  $27\mu\text{cm}^{-2}$ . The Smith term arises from the sample disorder and contributes both a downturn in  $\Delta\sigma_1$  and a negative  $\Delta\sigma_2$  at the lowest frequencies [67].

photonics, wavefront control, and short-range wireless THz communication applications [61], [83], [84].

However, it is very difficult to produce a dynamic response in flexible photonic gadgets. In [86] experimentally prove that the solution of perovskite with an intrinsic ultrafast response could be an ideal platform for developing active flexible photonic devices. A novel silicon-contained THz metallic split-ring metamaterial is proposed in [87]. The Fano resonance and transmission can be controlled through external biasing. Fano resonance and transmission amplitude abate drastically with the rise of current bias. As the current bias is increased, both the thickness and conductivity of the silicon carrier layer are modulated simultaneously.

Transition metal dichalcogenides (TMDs) consist of transition metal atoms covalently bonded to chalcogens (S, Se, or Te) to form atomic trilayers [89]. Although TMDs are appropriate for innovative THz devices, their performance in the THz range has only been studied in a few papers in the literature [90], [91], [92]. Molybdenum disulfide ( $\text{MoS}_2$ ) is already showing promise for use in electronic and photonic devices [93], [94], [95], [96]. The lattice and band structures


**FIGURE 10.** (a) THz radiation in reflection configuration.  $XYZ$  and  $X'Y'Z'$  represent the laboratory and crystal coordinate, respectively. Generated THz pulses in (b) time and domain from layered  $\text{MoS}_2$  (red solid curve), graphite (blue dash curve), and  $\text{InAs}$  crystal (black dash curve) [85].

of monolayer  $\text{MoS}_2$  are shown Fig. 5 d.  $\text{MoS}_2$  belongs to the family of 2D layered TMDs [97], [98]. Ultrafast carrier dynamics in monolayer and trilayer  $\text{MoS}_2$  and  $\text{WSe}_2$  were observed using time-resolved photoluminescence and THz spectroscopy [99]. The ultrafast reaction time of photoconductivity and photoluminescence in the monolayer  $\text{MoS}_2$  is 350 fs, while it is 1 ps in the trilayer  $\text{MoS}_2$  and monolayer  $\text{WSe}_2$ . These findings demonstrate the enormous potential of these materials for use in high-speed THz devices [100]. Recently, a monolayer of  $\text{MoS}_2$ , such as monolayer  $\text{MoS}_2$  nanostructure, have become potential materials of SPPs due to direct bandgap and strong spin-orbit couplings, which can effectively reduce losses of SPPs. Moreover,  $\text{MoS}_2$  nanostructure exhibits excellent photoelectric properties and has been suggested to be used in field effect transistors [26].

Measurement of ultrafast charge carrier dynamics in monolayers and trilayers of TMDs ( $\text{MoS}_2$ ) and  $\text{WSe}_2$  using a combination of time-resolved photoluminescence and THz spectroscopy showed the possibility of TMDs as high-speed optoelectronic [99].  $\text{MoS}_2$  can produce THz radiation with a linearly polarized femtosecond laser [85]. The radiated THz amplitude of  $\text{MoS}_2$  has a linear dependence on ever-increasing pump fluence and thus quadratic with the pump electric field.

Controlling the propagation of THz waves is very important in THz technologies, practically in high-speed communication. An optically tunable THz modulator using multilayer- $\text{MoS}_2$  and a silicon substrate are presented in [101]. The modulator shows higher modulation efficiency

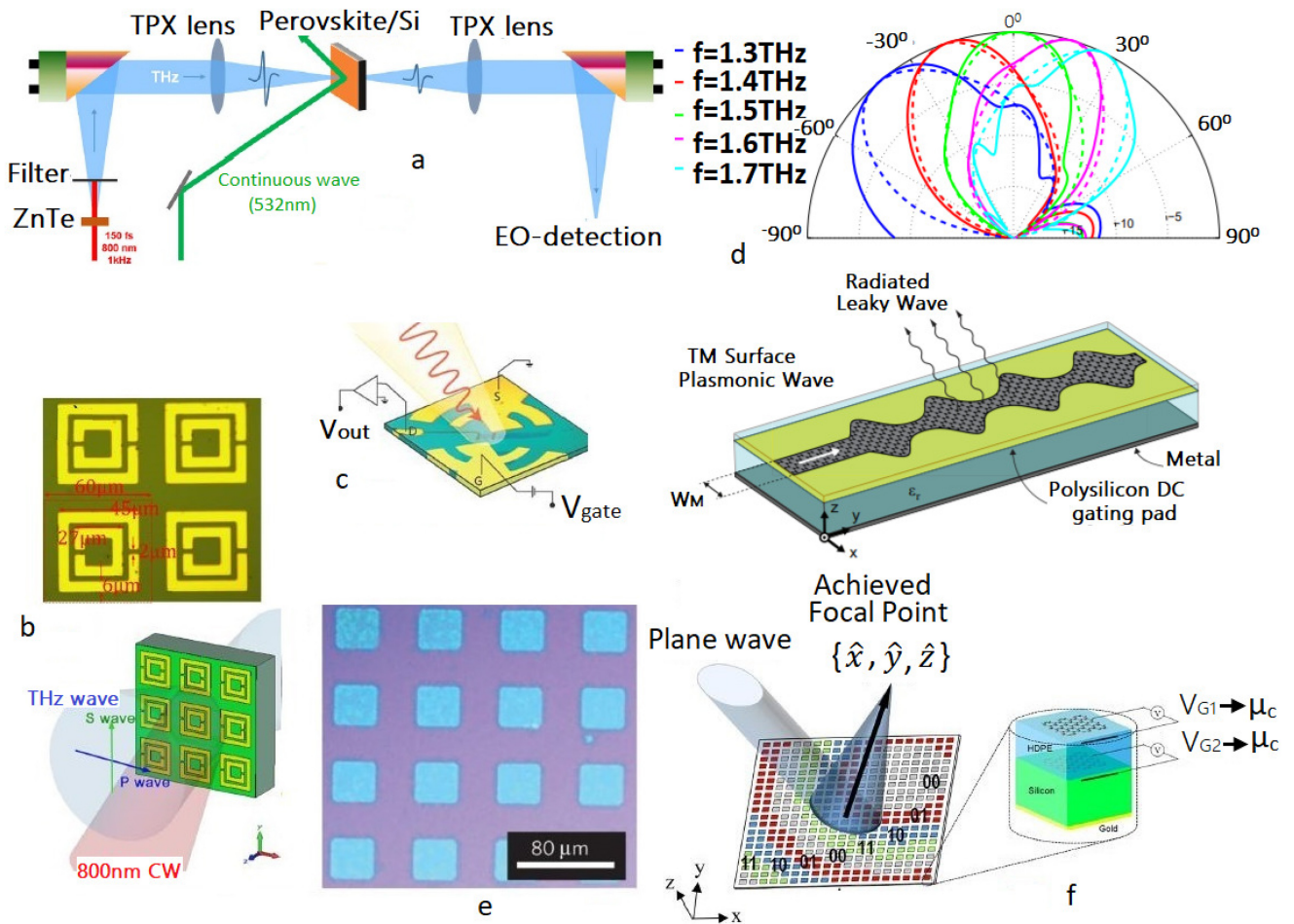


**FIGURE 11.** THz devices based on 2DMs. (a) Schematic of optically controllable THz modulation using perovskite and silicon [79]. (b) A MoS<sub>2</sub> metasurface [75]. (c) A three-dimensional model of Graphene field-effect transistors as room-temperature terahertz detectors [73]. (d) A non-reciprocal leaky-wave antenna based on a spatiotemporally variable surface impedance made of graphene [73]. (e) A MoS<sub>2</sub> growth in a CVD process as seen in an optical microscope [88]. (f) A flat mirror coding metasurface with adjustable focus [72].

than the graphene modulator. An alternative mechanism for modulating the emission from a quantum-cascade laser (QCL) device in which optically generated acoustic phonon pulses are used to perturb the QCL band structure, enabling fast amplitude modulation that can be controlled using the QCL drive current or strain pulse amplitude, up to a modulation depth of 6% [102].

In [103] design based on MoS<sub>2</sub>, the mid-infrared to THz can be realized. A MoS<sub>2</sub> layer between 200 nm diameter gold nanoparticle (AuNP) and 150 nm gold film is enhanced by more than four times compared with the bare MoS<sub>2</sub> sample. The implications of these atomic-scale hybrid materials could be revolutionary for THz applications.

The potential THz applications of 2D materials: Graphene and beyond are shown in Table 1.

### III. 2D MATERIAL THZ APPLICATION

With the fast advancement of graphene and other 2DMs, it is possible to increase the 2DMs' THz responsiveness and regulate THz waves. Many THz devices can be made

because of the large variety of material characteristics and the ability to combine 2DMs in a hybrid construction. In Fig. 11 (a), Hybrid silicon-perovskite structures are proposed for optically controlled THz wave switching between 0.2 and 2 THz. The THz amplitude modulation was controlled by using a 532 nm external laser to generate free carriers. Perovskite and silicon in a one-step manufacturing technique showed excellent stability and modulation efficiency. With this configuration, a THz switch could be achievable [79]. The progress on 2DMs such as graphene and MoS<sub>2</sub> materials offers a different research idea for THz modulator, an optically pumped THz modulator based on a MoS<sub>2</sub> and silicon meta surface are fabricated in [75]. It has been shown that graphene can be utilized to actively manipulate the waveguide characteristics. A simple straight waveguide coated with graphene can combine the comparatively low loss of silicon waveguides with the ultra-rapid tuning of graphene electromagnetic characteristics at THz frequencies [104]. The THz wave modulation based on MoS<sub>2</sub> metasurface has been demonstrated experimentally using

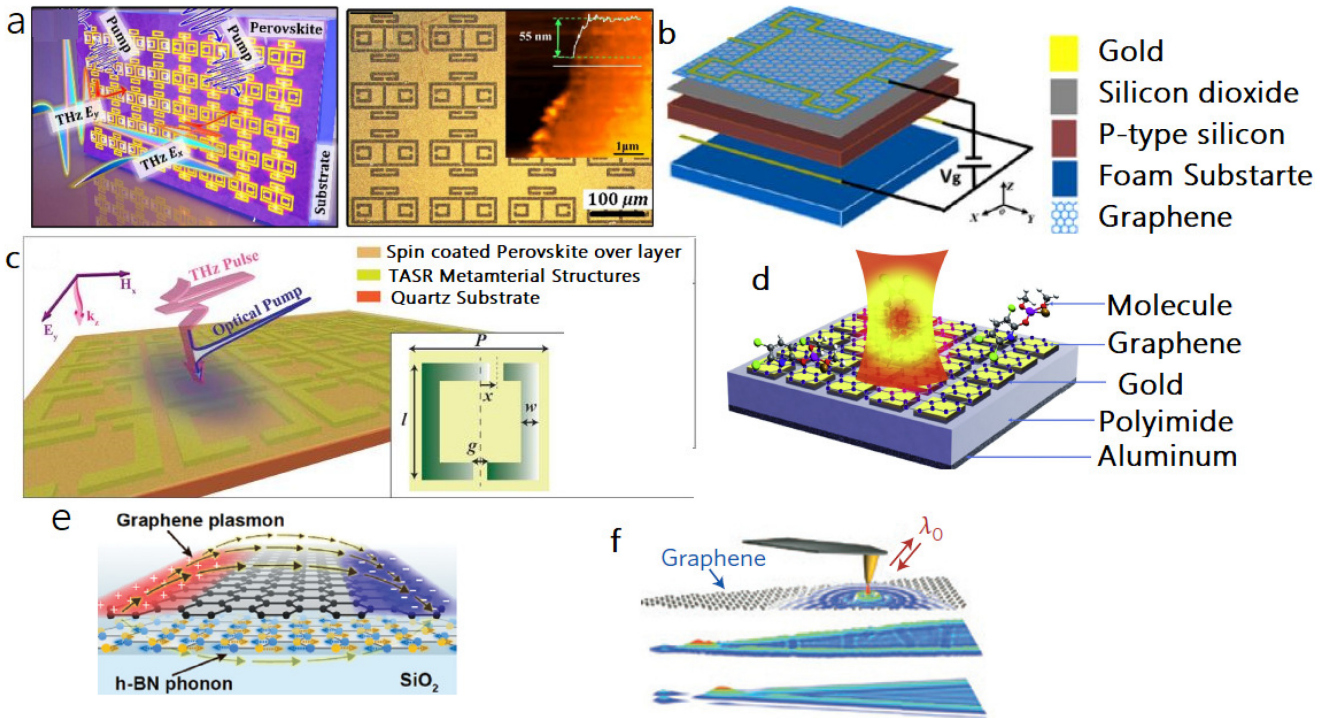


**FIGURE 12.** (a) Schematic diagram of the polarization-dependent metamaterial perovskite THz device [80]. (b) An active frequency selective surface for angle beam steering based on a hybrid graphene-gold structure [105]. (c) The perovskite-coated hybrid metadvice is shown in an artistic manner, with the 2D perovskite spin-coated (thickness 60 nm) on top of THz asymmetric split ring (TASR) and photoexcited using a 400-nm optical pump beam with THz as the probe [61]. (d) Optical microscope images of the constructed planar TASR metamaterial structure [71]. (e) H-BN monolayer sheet is used to construct graphene nanoresonators on Si wafer [81]. (f) Experimentation using a scanning near-field optical microscope tip to initiate plasmon-polariton waves in a graphene wedge [106].

time-domain spectroscopy and, which can reach over 90% under the incident wave laser pumping of  $4 \text{ W/cm}^2$  power density. A metasurface of the construction of the double split ring resonator is shown in Fig. 11 b. The metallic metal surface structure's resonances divide the modulation spectrum into a number of different frequency windows. By manipulating the geometric structure of the meta surface and incident polarization, the modulation spectrum's frequency, position, and bandwidth may be altered. In terms of wireless communication, graphene has extraordinary potential for short-range THz wireless communication. This feature enables the use of THz wireless technology in integrated systems where conventional metals are incompatible. It was shown that the graphene electrical field effect may be used to efficiently tune the antenna's frequency. The suggested strategy and approaches are critical for addressing the contemporary and basic challenges of excitation detection. In Figure 11 (d), based on the periodic modulation of a graphene strip, researchers have converted plasmons to free space waves. Analyze the dispersion, forecast the connection efficiency and emitted field, and build strip structures capable of meeting precise coupling requirements [74]. In [73] (Fig. 11 (c)), the study illustrates THz detectors based on antenna-coupled graphene field effect transistors. These use the nonlinear response of the gate to the radiation field, with thermoelectric and photoconductive origins, to enable large-area, rapid imaging of macroscopical materials.

Figure 11 (e), a straightforward method to grow large-area  $\text{MoS}_2$  films with controlled nucleation and promote the formation of large-area films formed by monolayer or few layers. In [88] used patterned substrates with the distribution of  $\text{SiO}_2$  pillars for  $\text{MoS}_2$  growth in the chemical vapour deposition (CVD) process.

The small loss in graphene plasmons at THz band is the main motivation for developing several waves tunable devices. A flat reflective which can be programmed to concentration THz waves to a certain point in the near field is proposed in [72] Fig. 11. (f). The reprogramming capability of the meta-mirror could be a key to improve compact THz scanning and imaging and novel reconfigurable component THz wireless communications. The device is conceived as a 2-bit coding metasurface that leverages the tunability of its graphene-based unit cells to control both the position and depth of focus.

Anisotropic optoelectronic devices have appeared as a desirable and attractive exploration subject owing to the latest developments in photonics technology involving communication and sensing. This is shown by a number of recent studies in photonics and optoelectronics, from solar cells and light-emitting devices to touch screens and photodetectors. 2D materials also cause ultrafast lasers to be on the rise [107]. Figure 12. (a), illustrates a framework for ultrasensitive and THz modulation of an efficient metamaterial device by creating an anisotropic perovskite-hybridized



resonator array [80]. A periodic array of closed-ring and split-ring resonators (CRRs and SRRs) is used to customize the plasmon-induced transparency (PIT) resonance at different frequencies determined by incident polarizations. On the quartz wafer, a thin layer of perovskite is deposited, which acts as a photoactive layer when irradiated with 400 nm optical pump pulses. Photo-swapping of Fano resonance-based subwavelength metamaterial devices at THz band may be enabled by using a hybrid lead halide perovskite solution as an active material. In [61] (Fig. 12 C), Lead halide perovskites are employed to determine a hybrid perovskite metamaterial device that exploits power photo switching of the metamaterial resonances in the THz band. In terms of antennas, much research has been undertaken to optimise the installation of THz antennas within environmental constraints. At THz frequencies, however, attaining significant angle steering for reconfigurable antennas remains a challenge. In [105] Fig. 12(b), the use of a gold and graphene-based construction to steer a 360-degree beam-steering THz antenna is discussed. With its adjustable beam direction and strength level, this antenna might be used for reconfigurable short-range THz wireless communication. Measurements of nanoresonators, which allow for hybridization with the phonons of the atomically thin h-BN layer to create two clearly separated new surface phonon plasmon-polariton (SPPP) modes with widths ranging from 30 to 300 nm, provide the electromagnetically coupled graphene plasmon/h-BN phonon mode frequency wavevector dispersion relations. in Fig. 12 (e). More studies into graphene plasmon-induced single-molecule excitation will benefit from the discovery that graphene nanoresonators may be utilized as extraordinarily sensitive probes [81].

In [71], integrated monolayer graphene on a metamaterial absorber cavity in which sensing targets induce a considerable shift in metamaterial resonant absorption or reflection owing to their high interaction with graphene. (Fig. 12 (d)). Scannable near-field optical microscopy tips are another new method for igniting graphene plasmons, Fig. 12 (f). A THz metamaterial absorber cavity integrates monolayer graphene, where the strong interaction between graphene and the sensing targets results in a substantial shift in metamaterial resonant absorption (or reflection). Graphene plasmon polaritons are excited when an infrared beam shines on a nanoscale metallic tip. The tip provides the extra momentum needed for this process. Reflections at the graphene edges cause standing-wave patterns [106].

A new generation of wireless communication is possible because of the fast development of 2D materials in recent years. The 2DM family exhibits a broad range of unique mechanical and electrical characteristics, such as thermal stability, bandgap tunability, and high conductivity, among other features. In addition, the ultra-high specific surface areas of 2DMs, in sharp contrast to their bulk counterparts, make their energy architecture sensitive to voltage biasing. Light-matter interactions can be dynamically controlled thanks to

graphene's exceptional electrical and optical characteristics in the THz range. A lot more research into the potential of TMDs and perovskites for THz applications is expected to lead to the discovery of numerous new and exciting terahertz phenomena and high-performance terahertz devices that are not yet possible with conventional technology. Both materials may be used to create terahertz modulators, detectors, polarizers, and absorbers. There are, however, a large number of 2DMs that have yet to be found. However, countless other 2DMs remain unknown. Additionally, mixing several 2DMs resulted in the formation of novel structures with distinct physical and concoction characteristics. Two-dimensional nanostructures are projected to be extremely compatible with existing microfabrication processes and to be readily integrated into metamaterials in the future. We propose that new strategies for scaling and transferring 2D materials should be developed. Controlling the layer count, domain size, and doping level of two-dimensional materials. The ability to design innovative functionalities and distinctive characteristics into 2D material tunnel devices enables the development of wearable THz devices such as antennas, sensors, and detectors for short-range wireless communication. It should be mentioned that the active study and development of two-dimensional materials are still in their infancy. When we examine the history of science and technology, we see that each stratum is mostly identical in that development was usually slow and laborious, and it took time for the most sophisticated materials to find commercial use.

#### IV. CONCLUSION

Terahertz communication literature is mostly focused on device technology. However, there is still a limited amount of research on the communication components required to construct Terahertz communication networks with a high bandwidth. Each scenario has its own set of difficulties. Metal THz antennas encounter a number of challenges, ranging from microfabrication to nanoscale electromagnetic interaction. Two-dimensional materials are showing promise as THz wireless device materials. Similarly, unique THz signal modulation devices based on upcoming technologies such as graphene have been proposed for use in short-range indoor communication. At THz frequencies, the key difficulty is getting efficient sources. Even with significant air attenuation, QCL may be a viable THz source of communication in the upper THz range. According to the several ways reported in the literature for obtaining THz sources. Recent developments in two-dimensional material (2DM) processing and fabrication points to a bright future towards the realisation of efficient terahertz sensing devices. This is, without doubt, the most critical component of an adequate THz technology for applications in future wireless communication systems. In this paper, we have reviewed various types of material properties in the THz band, and some of them can provide high conductivity, which is required in THz wireless communications. Reviewing recent work

on 2DMs reveals that improved methods in terms of fabrication and measurement are required. 2DMs have a lot of advantages, including lightweight, flexibility, electrical characteristics, and environmental friendliness. 2DM can be ideal with THz wearable devices. On the contrary, a fundamental disadvantage of 2DMs is their high absorption. Finally, it is concluded that the current technology needs to be further developed in the years to come and many problems related to the THz communication system need to be solved.

## REFERENCES

- [1] A. H. Lettington, I. M. Blankson, M. F. Attia, and D. Dunn, "Review of imaging architecture," in *Proc. Infrared Passive Millimeter-Wave Imag. Syst. Des. Anal. Model. Test.*, vol. 4719, 2002, pp. 327–340.
- [2] A. Rogalski and F. Sizov, "Terahertz detectors and focal plane arrays," *Opto-Electron. Rev.*, vol. 19, no. 3, pp. 346–404, 2011.
- [3] F. F. Sizov, "Infrared and terahertz in biomedicine," *Semicond. Phys. Quantum Electron. Optoelectron.*, vol. 3, no. 20, pp. 273–283, 2017.
- [4] D. Saeedkia, *Handbook of Terahertz Technology for Imaging, Sensing and Communications*, Elsevier, 2013.
- [5] R. Piesiewicz *et al.*, "Short-range ultra-broadband terahertz communications: Concepts and perspectives," *IEEE Antennas Propag. Mag.*, vol. 49, no. 6, pp. 24–39, Dec. 2007.
- [6] T. Kleine-Ostmann and T. Nagatsuma, "A review on terahertz communications research," *J. Infrared Millimeter THz Waves*, vol. 32, no. 2, pp. 143–171, 2011.
- [7] C. A. Balanis, *Antenna Theory: Analysis and Design*. Hoboken, NJ, USA: Wiley, 2016.
- [8] A. Hocini, M. N. Temmar, D. Khedrouche, and M. Zamani, "Novel approach for the design and analysis of a terahertz microstrip patch antenna based on photonic crystals," *Photon. Nanostruct. Fundam. Appl.*, vol. 36, Sep. 2019, Art. no. 100723.
- [9] M. Koch, "Terahertz communications: A 2020 vision," in *Terahertz Frequency Detection and Identification of Materials and Objects*. Dordrecht, The Netherlands: Springer, 2007, pp. 325–338.
- [10] S. J. Kim, K. Choi, B. Lee, Y. Kim, and B. H. Hong, "Materials for flexible, stretchable electronics: Graphene and 2D materials," *Annu. Rev. Mater. Res.*, vol. 45, pp. 63–84, Jul. 2015.
- [11] S. Ghafoor, M. H. Rehmani, and A. Davy, *Next Generation Wireless Terahertz Communication Networks*. Boca Raton, FL, USA: CRC Press, 2021.
- [12] G. W. Hanson, "Fundamental transmitting properties of carbon nanotube antennas," *IEEE Trans. Antennas Propag.*, vol. 53, no. 11, pp. 3426–3435, Nov. 2005.
- [13] G. Y. Slepyan, S. A. Maksimenko, A. Lakhtakia, O. Yevtushenko, and A. V. Gusakov, "Electrodynamics of carbon nanotubes: Dynamic conductivity, impedance boundary conditions, and surface wave propagation," *Phys. Rev. B, Condens. Matter*, vol. 60, no. 24, 1999, Art. no. 17136.
- [14] M. Walther, D. G. Cooke, C. Sherstan, M. Hajar, M. R. Freeman, and F. A. Hegmann, "Terahertz conductivity of thin gold films at the metal-insulator percolation transition," *Phys. Rev. B, Condens. Matter*, vol. 76, no. 12, 2007, Art. no. 125408.
- [15] T. Thio, H. F. Ghaemi, H. J. Lezec, P. A. Wolff, and T. W. Ebbesen, "Surface-plasmon-enhanced transmission through hole arrays in Cr films," *J. Opt. Soc. Amer. B*, vol. 16, no. 10, pp. 1743–1748, 1999.
- [16] S. S. Dhillon *et al.*, "The 2017 terahertz science and technology roadmap," *J. Phys. D, Appl. Phys.*, vol. 50, no. 4, 2017, Art. no. 043001.
- [17] T. Hochrein, "Markets, availability, notice, and technical performance of terahertz systems: Historic development, present, and trends," *J. Infrared Millimeter THz Waves*, vol. 36, no. 3, pp. 235–254, 2015.
- [18] K.-E. Peiponen, A. Zeitler, and M. Kuwata-Gonokami, *Terahertz Spectroscopy and Imaging*, vol. 171. Heidelberg, Germany: Springer, 2012.
- [19] M. Long, P. Wang, H. Fang, and W. Hu, "Progress, challenges, and opportunities for 2D material based photodetectors," *Adv. Funct. Mater.*, vol. 29, no. 19, 2019, Art. no. 1803807.
- [20] P. Gopalan and B. Sensale-Rodriguez, "2D materials for terahertz modulation," *Adv. Opt. Mater.*, vol. 8, no. 3, 2020, Art. no. 1900550.
- [21] L. Sun, W. Wang, and H. Yang, "Recent progress in synaptic devices based on 2D materials," *Adv. Intell. Syst.*, vol. 2, no. 5, 2020, Art. no. 1900167.
- [22] Y. Zhang *et al.*, "Broadband and tunable high-performance microwave absorption of an ultralight and highly compressible graphene foam," *Adv. Mater.*, vol. 27, no. 12, pp. 2049–2053, 2015.
- [23] R. Mas-Ballesté, C. Gómez-Navarro, J. Gómez-Herrero, and F. Zamora, "2D materials: To graphene and beyond," *Nanoscale*, vol. 3, no. 1, pp. 20–30, 2011.
- [24] A. Chaves *et al.*, "Bandgap engineering of two-dimensional semiconductor materials," *NPJ 2D Mater. Appl.*, vol. 4, no. 1, pp. 1–21, 2020.
- [25] E. Lee, Y. S. Yoon, and D.-J. Kim, "Two-dimensional transition metal dichalcogenides and metal oxide hybrids for gas sensing," *ACS Sens.*, vol. 3, no. 10, pp. 2045–2060, 2018.
- [26] A. Baron, S. Larouche, D. J. Gauthier, and D. R. Smith, "Scaling of the nonlinear response of the surface plasmon polariton at a metal/dielectric interface," *J. Opt. Soc. Amer. B*, vol. 32, no. 1, pp. 9–14, 2015.
- [27] J. Liu, Z. U. Khan, and S. Sarjoghian, "Layered THz waveguides for SPPs, filter and sensor applications," *J. Opt.*, vol. 48, no. 4, pp. 567–581, 2019.
- [28] A. Abohmrá *et al.*, "An ultrawideband microfabricated gold-based antenna array for terahertz communication," *IEEE Antennas Wireless Propag. Lett.*, vol. 20, pp. 2156–2160, 2021.
- [29] A. I. Fernández-Domínguez, E. Moreno, L. Martín-Moreno, and F. J. García-Vidal, "Terahertz wedge plasmon polaritons," *Opt. Lett.*, vol. 34, no. 13, pp. 2063–2065, 2009.
- [30] P. Tassin, T. Koschny, M. Kafesaki, and C. M. Soukoulis, "A comparison of graphene, superconductors and metals as conductors for metamaterials and plasmonics," *Nat. Photon.*, vol. 6, no. 4, pp. 259–264, 2012.
- [31] K. S. Novoselov, O. A. Mishchenko, O. A. Carvalho, and A. H. C. Neto, "2D materials and van der waals heterostructures," *Science*, vol. 353, no. 6298, p. aac9439, 2016.
- [32] T. Gould, S. Lebègue, T. Bjorkman, and J. F. Dobson, "2D structures beyond graphene: The brave new world of layered materials and how computers can help discover them," *Semicond. Semimetals*, vol. 95, pp. 1–33, Jan. 2016.
- [33] P. Miró, M. Audiffred, and T. Heine, "An atlas of two-dimensional materials," *Chem. Soc. Rev.*, vol. 43, no. 18, pp. 6537–6554, 2014.
- [34] C. L. Holloway, E. F. Kuester, J. A. Gordon, J. O'Hara, J. Booth, and D. R. Smith, "An overview of the theory and applications of metasurfaces: The two-dimensional equivalents of metamaterials," *IEEE Antennas Propag. Mag.*, vol. 54, no. 2, pp. 10–35, Apr. 2012.
- [35] B. Kapilevich, Y. Pinhasi, and B. Litvak, "Application of the matched THz power meter for material characterization in free space," in *Proc. IEEE Int. Conf. Microw. Commun. Antennas Electron. Syst. (COMCAS)*, Tel Aviv, Israel, 2011, pp. 1–4.
- [36] G. W. Hanson, "Radiation efficiency of nano-radius dipole antennas in the microwave and far-infrared regimes," *IEEE Antennas Propag. Mag.*, vol. 50, no. 3, pp. 66–77, Jun. 2008.
- [37] A. Ahmadi and H. Mosallaei, "Physical configuration and performance modeling of all-dielectric metamaterials," *Phys. Rev. B, Condens. Matter*, vol. 77, no. 4, 2008, Art. no. 045104.
- [38] G.-H. Lee *et al.*, "Electron tunneling through atomically flat and ultrathin hexagonal boron nitride," *Appl. Phys. Lett.*, vol. 99, no. 24, 2011, Art. no. 243114.
- [39] C. R. Dean *et al.*, "Boron nitride substrates for high-quality graphene electronics," *Nat. Nanotechnol.*, vol. 5, no. 10, pp. 722–726, 2010.
- [40] C. R. Dean *et al.*, "Hofstadter's butterfly and the fractal quantum hall effect in moiré superlattices," *Nature*, vol. 497, no. 7451, pp. 598–602, 2013.
- [41] L. Britnell *et al.*, "Field-effect tunneling transistor based on vertical graphene heterostructures," *Science*, vol. 335, no. 6071, pp. 947–950, 2012.
- [42] Y. Hernandez *et al.*, "High-yield production of graphene by liquid-phase exfoliation of graphite," *Nat. Nanotechnol.*, vol. 3, no. 9, pp. 563–568, 2008.
- [43] S. Nakamura *et al.*, "Ingan-based multi-quantum-well-structure laser diodes," *Jpn. J. Appl. Phys.*, vol. 35, no. 1B, p. L74, 1996.
- [44] Y. Huang, W.-Y. Yin, and Q. H. Liu, "Performance prediction of carbon nanotube bundle dipole antennas," *IEEE Trans. Nanotechnol.*, vol. 7, no. 3, pp. 331–337, May 2008.

- [45] T. Seifert *et al.*, "Efficient metallic spintronic emitters of ultrabroadband terahertz radiation," *Nat. Photon.*, vol. 10, no. 7, pp. 483–488, 2016.
- [46] N. Laman and D. Grischkowsky, "Terahertz conductivity of thin metal films," *Appl. Phys. Lett.*, vol. 93, no. 5, 2008, Art. no. 051105.
- [47] L. Ju *et al.*, "Graphene plasmonics for tunable terahertz metamaterials," *Nat. Nanotechnol.*, vol. 6, no. 10, pp. 630–634, 2011.
- [48] J. Liu, Z. U. Khan, C. Wang, H. Zhang, and S. Sarjoghian, "Review of graphene modulators from the low to the high figure of merits," *J. Phys. D, Appl. Phys.*, vol. 53, no. 23, 2020, Art. no. 233002.
- [49] S. Singha, "CPW fed jasmine shaped superwideband terahertz antenna for pattern diversity applications," *Optik*, vol. 231, Apr. 2021, Art. no. 166356.
- [50] X. Li *et al.*, "Graphene and related two-dimensional materials: Structure-property relationships for electronics and optoelectronics," *Appl. Phys. Rev.*, vol. 4, no. 2, 2017, Art. no. 021306.
- [51] A. R. Davoyan, V. V. Popov, and S. A. Nikitov, "Tailoring terahertz near-field enhancement via two-dimensional plasmons," *Phys. Rev. Lett.*, vol. 108, no. 12, 2012, Art. no. 127401.
- [52] Y. Zhang, Y. Feng, B. Zhu, J. Zhao, and T. Jiang, "Graphene based tunable metamaterial absorber and polarization modulation in terahertz frequency," *Opt. Exp.*, vol. 22, no. 19, pp. 22743–22752, 2014.
- [53] M. Tamagnone *et al.*, "Near optimal graphene terahertz non-reciprocal isolator," *Nat. Commun.*, vol. 7, no. 1, pp. 1–6, 2016.
- [54] R. Yan, S. Arezoomandan, B. Sensale-Rodriguez, and H. G. Xing, "Exceptional terahertz wave modulation in graphene enhanced by frequency selective surfaces," *ACS Photon.*, vol. 3, no. 3, pp. 315–323, 2016.
- [55] A. Vakil and N. Engheta, "Transformation optics using graphene," *Science*, vol. 332, no. 6035, pp. 1291–1294, 2011.
- [56] S. Abadal, I. Llatser, A. Mestres, H. Lee, E. Alarcón, and A. Cabellos-Aparicio, "Time-domain analysis of graphene-based miniaturized antennas for ultra-short-range impulse radio communications," *IEEE Trans. Commun.*, vol. 63, no. 4, pp. 1470–1482, Apr. 2015.
- [57] I. Llatser Martí *et al.*, "Radiation characteristics of tunable graphenans in the terahertz band," *Radioengineering*, vol. 21, no. 4, pp. 1–8, 2012.
- [58] G. W. Hanson, "Dyadic green's functions and guided surface waves for a surface conductivity model of graphene," *J. Appl. Phys.*, vol. 103, no. 6, 2008, Art. no. 064302.
- [59] S. A. Mikhailov and K. Ziegler, "New electromagnetic mode in graphene," *Phys. Rev. Lett.*, vol. 99, no. 1, 2007, Art. no. 016803.
- [60] B. Guzelturk *et al.*, "Terahertz emission from hybrid perovskites driven by ultrafast charge separation and strong electron-phonon coupling," *Adv. Mater.*, vol. 30, no. 11, 2018, Art. no. 1704737.
- [61] A. Kumar *et al.*, "Excitons in 2D perovskites for ultrafast terahertz photonic devices," *Sci. Adv.*, vol. 6, no. 8, p. eaax8821, 2020.
- [62] A. Kulkarni *et al.*, "Mixed ionic electronic conducting perovskite anode for direct carbon fuel cells," *Int. J. Hydrogen Energy*, vol. 37, no. 24, pp. 19092–19102, 2012.
- [63] N. K. Noel *et al.*, "Enhanced photoluminescence and solar cell performance via lewis base passivation of organic-inorganic lead halide perovskites," *ACS Nano*, vol. 8, no. 10, pp. 9815–9821, 2014.
- [64] W.-J. Yin, T. Shi, and Y. Yan, "Unusual defect physics in CH<sub>3</sub>NH<sub>3</sub>PbI<sub>3</sub> perovskite solar cell absorber," *Appl. Phys. Lett.*, vol. 104, no. 6, 2014, Art. no. 063903.
- [65] M. A. Green, A. Ho-Baillie, and H. J. Snaith, "The emergence of perovskite solar cells," *Nat. Photon.*, vol. 8, no. 7, pp. 506–514, 2014.
- [66] A. Abohmrta, H. Abbas, S. F. Jilani, A. Alomainy, M. A. Imran, and Q. H. Abbasi, "High bandwidth perovskite based antenna for high-resolution biomedical imaging at terahertz," in *Proc. IEEE Int. Symp. Antennas Propag. USNC-URSI Radio Sci. Meeting*, Atlanta, GA, USA, 2019, pp. 503–504.
- [67] T. Salim *et al.*, "Elucidating the role of disorder and free-carrier recombination kinetics in CH<sub>3</sub>NH<sub>3</sub>PbI<sub>3</sub> perovskite films," *Nat. Commun.*, vol. 6, no. 1, pp. 1–8, 2015.
- [68] N. V. Smith, "Classical generalization of the drude formula for the optical conductivity," *Phys. Rev. B, Condens. Matter*, vol. 64, no. 15, 2001, Art. no. 155106.
- [69] M. Dragoman, A. A. Muller, D. Dragoman, F. Coccetti, and R. Plana, "Terahertz antenna based on graphene," *J. Appl. Phys.*, vol. 107, no. 10, 2010, Art. no. 104313.
- [70] I. Llatser, C. Kremers, A. Cabellos-Aparicio, J. M. Jornet, E. Alarcón, and D. N. Chigrin, "Graphene-based nano-patch antenna for terahertz radiation," *Photon. Nanostruct. Fundam. Appl.*, vol. 10, no. 4, pp. 353–358, 2012.
- [71] W. Xu *et al.*, "Terahertz biosensing with a graphene-metamaterial heterostructure platform," *Carbon*, vol. 141, pp. 247–252, Jan. 2019.
- [72] S. E. Hosseinejad *et al.*, "Reprogrammable graphene-based metasurface mirror with adaptive focal point for THz imaging," *Sci. Rep.*, vol. 9, no. 1, pp. 1–9, 2019.
- [73] L. Vicarelli *et al.*, "Graphene field-effect transistors as room-temperature terahertz detectors," *Nat. Mater.*, vol. 11, no. 10, pp. 865–871, 2012.
- [74] J. S. Gómez-Díaz, M. Esquiús-Morote, and J. Perruisseau-Carrier, "Plane wave excitation-detection of non-resonant plasmons along finite-width graphene strips," *Opt. Exp.*, vol. 21, no. 21, pp. 24856–24872, 2013.
- [75] W. Zheng, F. Fan, M. Chen, S. Chen, and S.-J. Chang, "Optically pumped terahertz wave modulation in MoS<sub>2</sub>-Si heterostructure metasurface," *AIP Adv.*, vol. 6, no. 7, 2016, Art. no. 075105.
- [76] Y. Huang *et al.*, "Terahertz surface emission from layered MoS<sub>2</sub> crystal: Competition between surface optical rectification and surface photocurrent surge," *J. Phys. Chem. C*, vol. 122, no. 1, pp. 481–488, 2018.
- [77] Y. Zhong *et al.*, "Tunable terahertz broadband absorber based on MoS<sub>2</sub> ring-cross array structure," *Opt. Mater.*, vol. 114, Apr. 2021, Art. no. 110996.
- [78] A. Abohmrta *et al.*, "Terahertz antenna array based on a hybrid perovskite structure," *IEEE Open J. Antennas Propag.*, vol. 1, pp. 464–471, 2020.
- [79] K.-S. Lee, R. Kang, B. Son, D.-Y. Kim, N. E. Yu, and D.-K. Ko, "All-optical THz wave switching based on CH<sub>3</sub>NH<sub>3</sub>PbI<sub>3</sub> perovskites," *Sci. Rep.*, vol. 6, 2016, Art. no. 37912.
- [80] J. Zhou *et al.*, "Ultrasensitive polarization-dependent terahertz modulation in hybrid perovskites plasmon-induced transparency devices," *Photon. Res.*, vol. 7, no. 9, pp. 994–1002, 2019.
- [81] V. W. Brar *et al.*, "Hybrid surface-phonon-plasmon polariton modes in graphene/monolayer h-BN heterostructures," *Nano Lett.*, vol. 14, no. 7, pp. 3876–3880, 2014.
- [82] Y. Rakita *et al.*, "Tetragonal CH<sub>3</sub>NH<sub>3</sub>PbI<sub>3</sub> is ferroelectric," *Proc. Nat. Acad. Sci.*, vol. 114, no. 28, pp. E5504–E5512, 2017.
- [83] A. Y. Pawar, D. D. Sonawane, K. B. Erande, and D. V. Derle, "Terahertz technology and its applications," *Drug Invention Today*, vol. 5, no. 2, pp. 157–163, 2013.
- [84] T. Yasuda, T. Yasui, T. Araki, and E. Abraham, "Real-time two-dimensional terahertz tomography of moving objects," *Opt. Commun.*, vol. 267, no. 1, pp. 128–136, 2006.
- [85] Y. Huang *et al.*, "Surface optical rectification from layered MoS<sub>2</sub> crystal by THz time-domain surface emission spectroscopy," *ACS Appl. Mater. Interfaces*, vol. 9, no. 5, pp. 4956–4965, 2017.
- [86] L. Cong, Y. K. Srivastava, A. Solanki, T. C. Sum, and R. Singh, "Perovskite as a platform for active flexible metaphotonic devices," *ACS Photon.*, vol. 4, no. 7, pp. 1595–1601, 2017.
- [87] J. Lou *et al.*, "Silicon-based terahertz meta-devices for electrical modulation of fano resonance and transmission amplitude," *Adv. Opt. Mater.*, vol. 8, no. 19, 2020, Art. no. 2000449.
- [88] S. Najmaei *et al.*, "Vapour phase growth and grain boundary structure of molybdenum disulphide atomic layers," *Nat. Mater.*, vol. 12, no. 8, pp. 754–759, 2013.
- [89] R. H. Friend and A. D. Yoffe, "Electronic properties of intercalation complexes of the transition metal dichalcogenides," *Adv. Phys.*, vol. 36, no. 1, pp. 1–94, 1987.
- [90] X. Hong *et al.*, "Ultrafast charge transfer in atomically thin MoS<sub>2</sub>/WS<sub>2</sub> heterostructures," *Nat. Nanotechnol.*, vol. 9, no. 9, pp. 682–686, 2014.
- [91] C.-H. Lee *et al.*, "Atomically thin p-n junctions with van der waals heterointerfaces," *Nat. Nanotechnol.*, vol. 9, no. 9, pp. 676–681, 2014.
- [92] M. M. Furchi, A. Pospischil, F. Libisch, J. Burgdörfe, and T. Mueller, "Photovoltaic effect in an electrically tunable van der waals heterojunction," *Nano Lett.*, vol. 14, no. 8, pp. 4785–4791, 2014.

- [93] K. S. Novoselov *et al.*, “Two-dimensional gas of massless dirac fermions in graphene,” *Nature*, vol. 438, no. 7065, pp. 197–200, 2005.
- [94] H. Wang *et al.*, “Integrated circuits based on bilayer MoS<sub>2</sub> transistors,” *Nano Lett.*, vol. 12, no. 9, pp. 4674–4680, 2012.
- [95] K. Kaasbjerg, K. S. Thygesen, and K. W. Jacobsen, “Phonon-limited mobility in *n*-type single-layer MoS<sub>2</sub> from first principles,” *Phys. Rev. B, Condens. Matter*, vol. 85, no. 11, 2012, Art. no. 115317.
- [96] H. Shi, H. Pan, Y.-W. Zhang, and B. I. Yakobson, “Quasiparticle band structures and optical properties of strained monolayer MoS<sub>2</sub> and WS<sub>2</sub>,” *Phys. Rev. B, Condens. Matter*, vol. 87, no. 15, 2013, Art. no. 15530.
- [97] Y. Kang *et al.*, “Plasmonic hot electron induced structural phase transition in a MoS<sub>2</sub> monolayer,” *Adv. Mater.*, vol. 26, no. 37, pp. 6467–6471, 2014.
- [98] L. Tao *et al.*, “1T’ transition metal telluride atomic layers for plasmon-free SERS at femtomolar levels,” *J. Amer. Chem. Soc.*, vol. 140, no. 28, pp. 8696–8704, 2018.
- [99] C. J. Docherty *et al.*, “Ultrafast transient terahertz conductivity of monolayer MoS<sub>2</sub> and WSe<sub>2</sub> grown by chemical vapor deposition,” *ACS Nano*, vol. 8, no. 11, pp. 11147–11153, 2014.
- [100] J. Shi *et al.*, “THz photonics in two dimensional materials and metamaterials: Properties, devices and prospects,” *J. Mater. Chem. C*, vol. 6, no. 6, pp. 1291–1306, 2018.
- [101] Y. Cao *et al.*, “Optically tuned terahertz modulator based on annealed multilayer MoS<sub>2</sub>,” *Sci. Rep.*, vol. 6, no. 1, pp. 1–9, 2016.
- [102] M. G. Ahangari, A. Salmankhani, A. H. Imani, N. Shahab, and A. H. Mashhadzadeh, “Density functional theory study on the mechanical properties and interlayer interactions of multilayer graphene: Carbonic, silicon-carbide and silicene graphene-like structures,” *Silicon*, vol. 11, no. 3, pp. 1235–1246, 2019.
- [103] L. Yu *et al.*, “Gap plasmon-enhanced photoluminescence of monolayer MoS<sub>2</sub> in hybrid nanostructure,” *Chin. Phys. B*, vol. 27, no. 4, 2018, Art. no. 047302.
- [104] A. Locatelli, G. E. Town, and C. De Angelis, “Graphene-based terahertz waveguide modulators,” *IEEE Trans. THz Sci. Technol.*, vol. 5, no. 3, pp. 351–357, May 2015.
- [105] B. Wu, Y. Hu, Y. T. Zhao, W. B. Lu, and W. Zhang, “Large angle beam steering THz antenna using active frequency selective surface based on hybrid graphene-gold structure,” *Opt. Exp.*, vol. 26, no. 12, pp. 15353–15361, 2018.
- [106] L. Deng *et al.*, “Manipulating of different-polarized reflected waves with graphene-based plasmonic metasurfaces in terahertz regime,” *Sci. Rep.*, vol. 7, no. 1, pp. 1–10, 2017.
- [107] F. Bonaccorso, Z. Sun, T. Hasan, and A. C. Ferrari, “Graphene photonics and optoelectronics,” *Nat. Photon.*, vol. 4, no. 9, pp. 611–622, 2010.